1800–1810 *Nucleic Acids Research, 2020, Vol. 48, No. 4* *Published online 13 January 2020*
doi: 10.1093/nar/gkz1172

Estrogen-induced transcription at individual alleles is independent of receptor level and active conformation but can be modulated by coactivators activity

Fabio Stossi[1,2,3,*], Radhika D. Dandekar[1,2], Maureen G. Mancini[1,3], Guowei Gu[1], Suzanne A.W. Fuqua[4,5], Agostina Nardone[4,5,6], Carmine De Angelis[4,5,6], Xiaoyong Fu[1,4], Rachel Schiff[1,4,5,6], Mark T. Bedford[7], Wei Xu[8], Hans E. Johansson[9], Clifford C. Stephan[10] and Michael A. Mancini[1,2,3,5,10,11]

[1]Department of Molecular and Cellular Biology, Baylor College of Medicine, Houston, TX 77030, USA, [2]Integrated Microscopy Core, Baylor College of Medicine, Houston, TX 77030, USA, [3]Gulf Coast Consortia Center for Advanced Microscopy and Image Informatics, Houston, TX 77030, USA, [4]Lester & Sue Smith Breast Center, Baylor College of Medicine, Houston, TX 77030, USA, [5]Dan L. Duncan Comprehensive Cancer Center, Baylor College of Medicine, Houston, TX 77030, USA, [6]Department of Medicine, Baylor College of Medicine, Houston, TX 77030, USA, [7]Department of Epigenetics and Molecular Carcinogenesis, The University of Texas MD Anderson Cancer Center, Smithville, TX 78957, USA, [8]McArdle Laboratory for Cancer Research, University of Wisconsin School of Medicine and Public Health, Madison, WI 53705, USA, [9]LGC Biosearch Technologies, Petaluma, CA 94954, USA, [10]Center for Translational Cancer Research, Institute of Biosciences and Technology, Texas A&M University, Houston, TX 77030, USA and [11]Department of Pharmacology and Chemical Biology, Baylor College of Medicine, Houston, TX 77030, USA

Received May 29, 2019; Revised November 29, 2019; Editorial Decision December 04, 2019; Accepted December 06, 2019

ABSTRACT

Steroid hormones are pivotal modulators of pathophysiological processes in many organs, where they interact with nuclear receptors to regulate gene transcription. However, our understanding of hormone action at the single cell level remains incomplete. Here, we focused on estrogen stimulation of the well-characterized GREB1 and MYC target genes that revealed large differences in cell-by-cell responses, and, more interestingly, between alleles within the same cell, both over time and hormone concentration. We specifically analyzed the role of receptor level and activity state during allele-by-allele regulation and found that neither receptor level nor activation status are the determinant of maximal hormonal response, indicating that additional pathways are potentially in place to modulate cell- and allele-specific responses. Interestingly, we found that a small molecule inhibitor of the arginine methyltransferases CARM1 and PRMT6 was able to increase, in a gene specific manner, the number of active alleles/cell before and after hormonal stimulation, suggesting that mechanisms do indeed exist to modulate hormone receptor responses at the single cell and allele level.

INTRODUCTION

Steroid hormones, like estrogen (E2), control a myriad of physiological processes. In target cells, they interact with nuclear receptors (e.g. estrogen receptor (ER)) and bind to specific DNA sequences that facilitate the recruitment of coregulator complexes to regulate gene transcription and establish/maintain cell phenotypes (1,2). Genome-wide studies have identified hundreds of ER target genes and thousands of ER binding sites on DNA (3–5), while other studies described scores of ER cofactors that impinge upon gene transcription (6,7). However, there is a paucity of information on how estrogen regulates transcription of endogenous genes at the level of individual cells, or individual target gene alleles. Recent studies have begun addressing this issue by single cell RNA-seq (8) and by dynamic live-imaging of an engineered model featuring CRISPRed-in MS2 repeat units at the TFF1 estrogen target gene (9), identifying novel descriptors of ER action such as pervasive, bimodal gene expression, and long refractory periods between transcriptional bursts. In recent years, the field of single cell gene transcription regulation (10–15) supports the notion of transcription as a stochastic phenomenon that in-

*To whom correspondence should be addressed. Tel: +1 713 798 6940; Fax: +1 713 790 1275; Email: stossi@bcm.edu

© The Author(s) 2020. Published by Oxford University Press on behalf of Nucleic Acids Research.
This is an Open Access article distributed under the terms of the Creative Commons Attribution Non-Commercial License (http://creativecommons.org/licenses/by-nc/4.0/), which permits non-commercial re-use, distribution, and reproduction in any medium, provided the original work is properly cited. For commercial re-use, please contact journals.permissions@oup.com

volves bursts of RNA synthesis of varied frequency and amplitude. Transcriptional bursting can be modulated by: cell volume (11), nuclear retention and transport of transcripts (16,17), mitochondrial content (18,19), enhancer strength and DNA looping (20), cell cycle (15), transcription factor levels and localization or signaling pathway activation (21–23). Compared with recent studies (8,9) that focused on either steady state or transcriptional bursting, we simultaneously analyzed both by using single molecule RNA FISH (smFISH) and image analysis. We report that E2 regulates target gene expression with heterogeneous responses in both a cell- and allele-specific manner based upon hormone dosage and length of exposure. This diverse response is maintained across cell lines with variable number of alleles and is also apparent for other steroid receptors (AR, GR and PR) and ligand classes (i.e. hormones, phytoestrogens, endocrine disruptors). By modulating ER levels (overexpression and knock-down), we show that very little ER is required for gene activation while the total level of the receptor per cell only minimally correlates with the number of active alleles. More interestingly, when all the cellular ER is rendered constitutively active by introducing the clinically relevant Y537S mutation (24), the allele-by-allele variability in response was preserved indicating that the activation status of ER is not the main determinant of allele-specific activation. With advances in genome-wide analysis by intron smFISH (25) it will soon be possible to have a complete picture of estrogen action on the nascent transcriptome at the single allele level. Finally, we propose that variation of allele-by-allele hormonal response can be modulated through coregulators, as we identified a small molecule inhibitor of CARM1/PRMT6 arginine methyltransferases (MS049) is capable of increasing the number of active alleles per cell both basally and under hormonal stimulation in a gene and cell type-specific manner.

MATERIALS AND METHODS

Cell culture

Cell lines (MCF-7, T47D, ZR-75-1, BT474, MCF-7/TamR) were obtained from BCM Cell Culture Core, which routinely validates their identity by genotyping, or ATCC. A validated ER-shRNA pGIPZ clone (V2LMM_136277, Open Biosystems, Huntsville, Al, USA) was used to construct a doxycycline (dox)-inducible pINDUCER-shER lentiviral vector, as previously described (50). Virus production, cell infection, selection, and induction of ER-shRNA in the stable MCF-7/ER-shRNA cells were performed as previously described (51). MCF-7/CARM1 KO cells were generated and obtained from Dr Xu (U. Wisconsin) and have been previously published (48). MCF-7/Y537S cells were generated and validated by Drs Gu and Fuqua, with the help from BCM C-BASS Core (manuscript in preparation). GFP-ERα:PRL-HeLa cells were previously described (46,47). All cell lines except the CARM1 KO tested mycoplasma negative as determined by DAPI staining. Cell lines were routinely maintained in their standard media, as recommended by ATCC, except phenol red free. Three days prior to experiments, cells were plated in media containing 5% charcoal–dextran stripped and dialyzed FBS-containing media.

Single molecule RNA FISH (smFISH)

Cells were fixed on ice in 4% purified formaldehyde (Electron Microscopy Sciences) in ribonuclease (RNase)-free PBS for 15 min, washed in PBS and then permeabilized with 70% ethanol in RNase-free water at 4°C for a minimum of 2 h. Cells were washed in 1 ml of wash buffer (2× saline sodium citrate [SSC] plus 10% formamide) followed by overnight hybridization with RNA FISH probes at 37C (Stellaris probes; LGC Biosearch Technologies) in hybridization buffer. Next, cells were rinsed in one change in wash buffer (30 min at 37°C), and a second wash in buffer containing 1 μg/ml DAPI (10 min at 37°C), as described (52) For experiments performed on poly-lysine coated coverslips, Vectashield (Vector Laboratories) was used as mounting medium, and sealed with nail polish. All probes were designed and synthesized by LGC Biosearch Technologies. Exon-probes (labeled with Quasar 570®) were custom designed against the common coding sequence of GREB1 mRNAs, using mRNA variant NM_014668.3, nts 143–457, 755–1459 as the defined target region (VSMF-2158-5). Intron probes (labeled with Quasar 670®) were designed against 7.5 kb of introns #4 to #10 (NG_029429.1). MYC probes were available as predesigned by LGC Biosearch Technologies.

Immunofluorescence and IF/FISH

Immunofluorescence experiments were completed as previously described (53). Briefly, cells were fixed in 4% formaldehyde in PBS, quenched with 0.1 M ammonium chloride for 10 min, and permeabilized with 0.5% Triton X-100 for 30 min. Cells were incubated at room temperature in blotto for 1 h, and then specific antibodies were added overnight at 4°C prior to 30 min of secondary antibody (AlexaFluor conjugates; Molecular Probes) and DAPI staining. The primary anti-ERα antibodies used were: mouse (in-house generated), rabbit (Millipore 04-820), and rat (H-222, Santa Cruz Biotechnology). The methyl MED12 (CARM1 methylation specific site) antibody was kindly provided by Dr Mark Bedford (UT-MD Anderson-Smithville).

The protocol for IF/FISH sequentially followed the IF protocol described above, except that 2× SSC was used instead of blotto and the primary and secondary antibodies incubations were for 1 h at 37°C and room temperature, respectively, and the dilution was increased to 1:500. After post-fix (4% PFA for 10 min), the samples were washed in RNA FISH wash buffer (LGC Biosearch Technologies) followed by hybridization with the FISH probes.

High resolution and high throughput microscopy

High quality/high resolution imaging was performed on a GE Healthcare DVLive epifluorescence image restoration microscope using an Olympus PlanApo 60×/1.42 NA objective and a 1.9k × 1.9k sCMOS camera. Z stacks (0.25 μm) covering the whole nucleus (~10 μm) were acquired before applying a conservative restorative algorithm for quantitative image deconvolution. Max intensity projections were generated and used for image analysis.

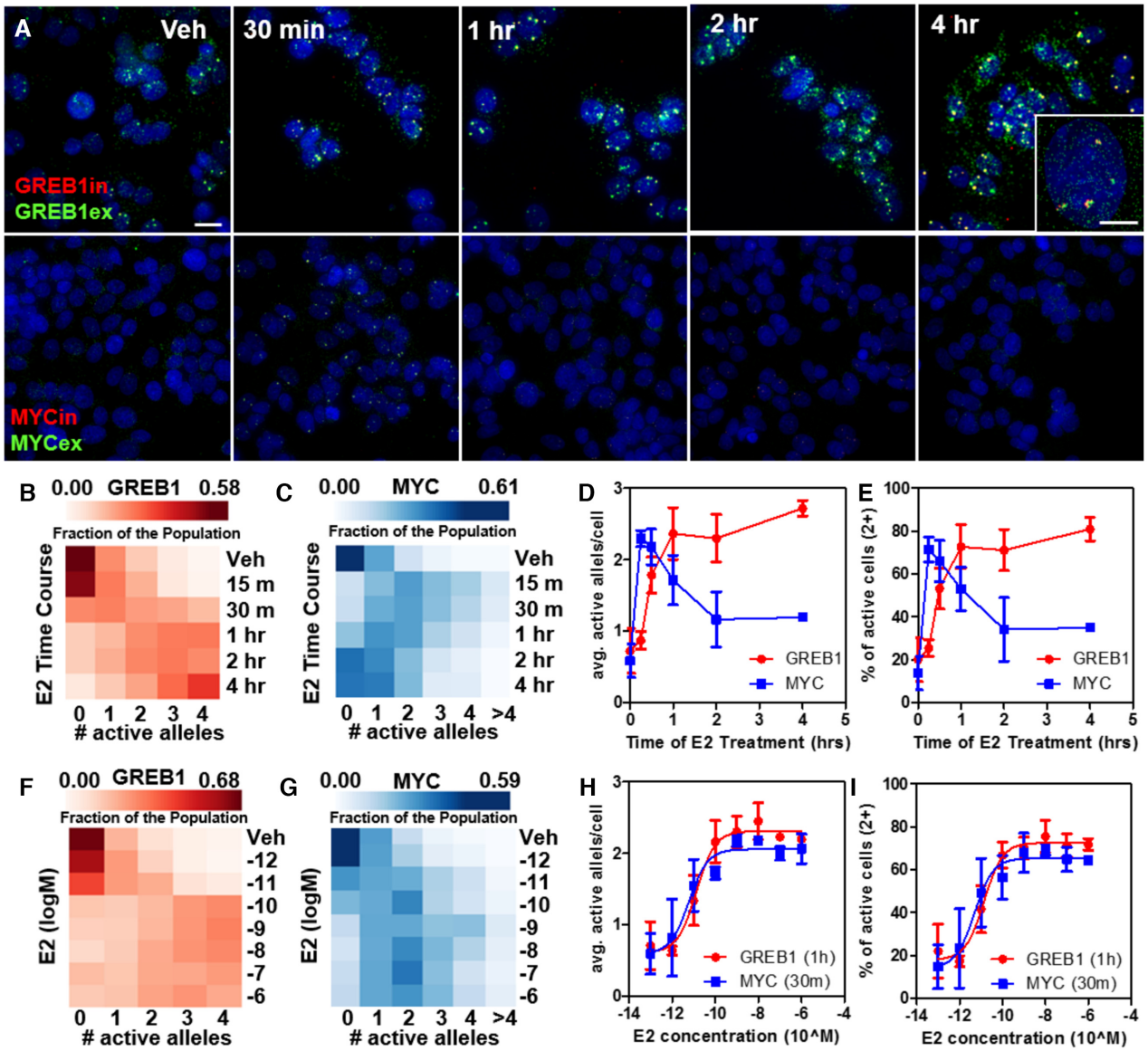

Figure 1. Cell-by-cell and allele-by-allele variation in estrogenic response. (**A**) Representative images of E2 treated MCF-7 cells over time, hybridized with probes detecting GREB1 (mature, GREB1ex, green; nascent, GREB1in, red), top panels, and MYC (mature, MYCex, green; nascent, MYCin, red), bottom panels, by single molecule RNA FISH. Scale bar: 10 μm. Inset shows a magnified cell (inset: 5 μm). (**B**, **C**) distribution of cells with 0–4 (or more in the case of MYC) active alleles, after E2 time course. (**D**–**H**) average number of active alleles in E2 time course and dose-response experiments. (**E**–**I**) fraction of activated cells (two or more active alleles) over time and dose of E2 treatment. (**F**–**G**) distribution of cells with 0–4 (or more for MYC) active alleles after E2 dose-response. >200 cells/treatment in ≥3 biological replicates.

Image and statistical analysis

Nuclear segmentation, spot identification, and intensity extraction were performed on maximum projection images using basic image analysis routines in Matlab, PipelinePilot (Biovia) (54), CellProfiler and Fiji. Apoptotic and mitotic cells were filtered out based on DAPI intensity and morphology. Visual inspection of the images validated counts of transcriptionally active alleles by determining overlap between exonic and intronic probe sets. Between 200 and 1000 cells/treatment/biological replicate were imaged and analyzed for the smFISH experiments, for IF studies, >1000 cells were analyzed. Every experiment was performed in two to four technical replicates and repeated for a minimum of three biological replicated. Only for visualization purposes, spots were enhanced by histogram stretching, equally across treatments, post acquisition in Fiji.

GraphPad Prism 5.0 was used to construct graphs and dose-response curves, calculate EC_{50}, and perform statistical tests. Data in every figure is either represented as median ± standard deviation or as box plots, with the box representing 25th to 75th percentile of the data. For multiple groups comparison, we used non-parametric Kruskal-Wallis test with Dunn's post test (significance level at 95% confidence); correlation analysis was done using Spearman's *r* (non parametric); while for comparing two groups

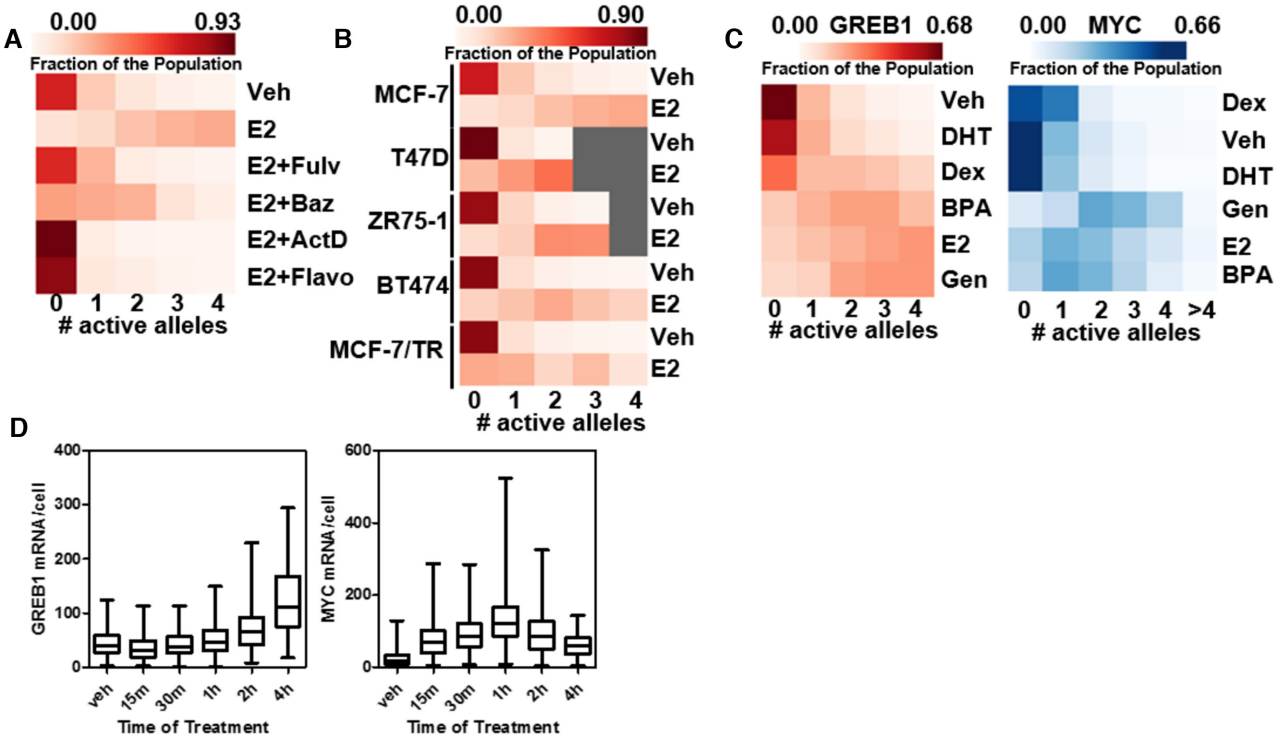

Figure 2. Allele-by-allele variation in response is independent of cell model, compound, and number of alleles. (**A**) MCF-7 cells were pretreated with fulvestrant (Fulv), bazedoxifene (Baz), actinomycin D (ActD) or flavopiridol (Flavo) for 1 h prior to addition of 10 nM of E2. Distribution of active GREB1 alleles is represented as heatmap. (**B**) The indicated cell lines were treated with E2 10 nM for 1 h prior to GREB1 smFISH. Gray boxes indicate that the particular cell line has a lower number of GREB1 alleles. (**C**) MCF-7 were treated for 1 h with E2 10 nM, dexamethasone (Dex, 100 nM), dihydroxytestosterone (DHT, 100 nM), bisphenol A (BPA, 1 μM), or genistein (GEN, 100 nM), and then smFISH was performed for GREB1 and MYC. (**D**) GREB1 and MYC exon probes smFISH was performed over an E2 time course in MCF-7 and individual mature RNAs/cell were counted and visualized by box-plot.

only, we used non-parametric *t*-test (Mann–Whitney test) reporting a two-tailed *P*-value. Heatmaps and hierarchical clustering was performed using Orange Data Mining (55).

RESULTS

Allele-by-allele regulation of E2 target genes in breast cancer cells

The Estrogen Receptor (ER) regulates hundreds of target genes with various response patterns (e.g. up- and down-regulated, time- and dose-dependent, (3,8,26)); however, less is known about hormonal actions at the single cell and, especially, at the level of individual alleles (8,9). We used smFISH to analyze the effects of the natural ER agonist, 17β-estradiol (E2), on two well-characterized ER target genes with different time courses of response and gene structure (GREB1 and MYC). GREB1 and MYC are ER primary target genes that are involved in cell proliferation and other cellular functions and have been shown to be stimulated with different time courses, GREB1 being sustained over time, while MYC being transient (3,26–28). GREB1 has also been used to predict ER-mediated phenotypic responses (29). We used spectrally-separated probe sets for each gene hybridizing to either intronic or exonic sequences (12) in order to quantify both nascent and mature RNA, with GREB1 being a long gene (>100 kb) that contains multiple introns, whereas MYC, being a short gene (∼4 kb), has only two introns. Visible overlap between the two probe sets was used to determine which alleles were active in every cell.

We treated synchronized (measured by EdU labeling after 48 h in charcoal-stripped media, not shown) MCF-7 breast cancer cells with 10 nM E2 for varying amounts of time (5 min to 4 h) to cover both early and sustained responses without impacting ER protein turnover and estrogen-mediated changes in cell cycle progression (Figure 1). Next, we counted the number of active alleles/cell and mature RNA/cell using semi-automated deconvolution microscopy and analysis (Figure 1A shows random fields for each gene target at each time point–GREB1 on top and MYC on bottom panels).

MCF-7 cells have four copies of chromosome 2 containing the GREB1 gene (30), while there are up to six copies of the MYC gene (31), hence a maximal response to E2 would result in four or more alleles being active in the same cell depending on the target gene. However, by counting overlapping intron and exon signals (i.e. transcriptionally active alleles), we observed that not all cells responded to hormone during the four hours of treatment (Figure 1), and clearly not all at the same time. From the acquired images (as seen in Figure 1A), a large variability in the number of active alleles is apparent within each nucleus. Analysis of the number of active alleles per cells shows a gene-specific shift

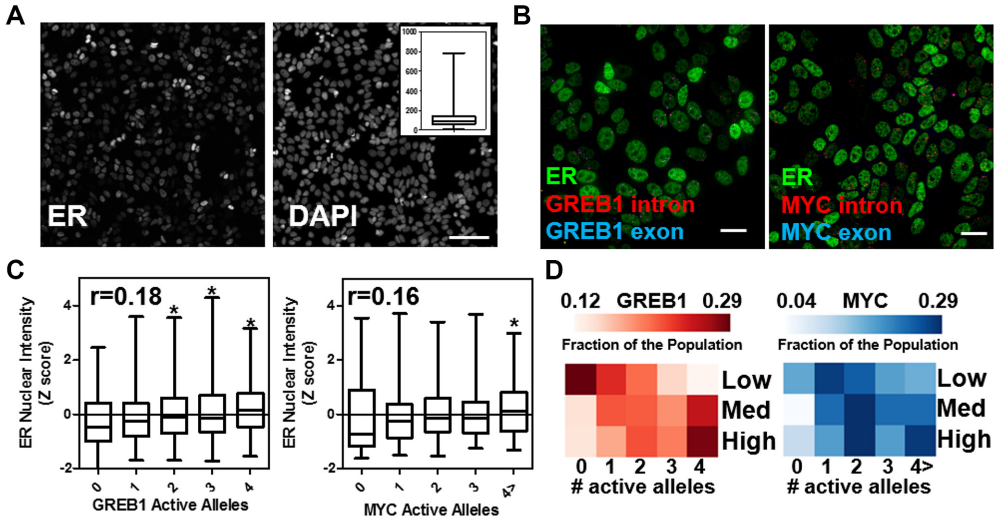

Figure 3. ER levels do not correlate with activation of GREB1 at the single cell level. (**A**) 20× image of ER immunofluorescence in MCF-7 cells. DAPI marks cell nuclei, scale bar is 100μm. Inset shows single cell quantitation of ER levels over >50 000 cells. (**B**) ER/GREB1 (intron + exon) and ER/MYC (intron + exon) IF/FISH 60× images (deconvolved and max projected) after 1 h of E2 treatment, scale bar is 20 μm. (**C**, **D**) Single cell analysis of experiments, as in panel B, where cells are stratified by either number of active alleles (C), or by ER levels (bottom 25th (low), 25th–75th (medium) and top 75th (high) percentiles) to show correlation between ER levels and transcriptional output.

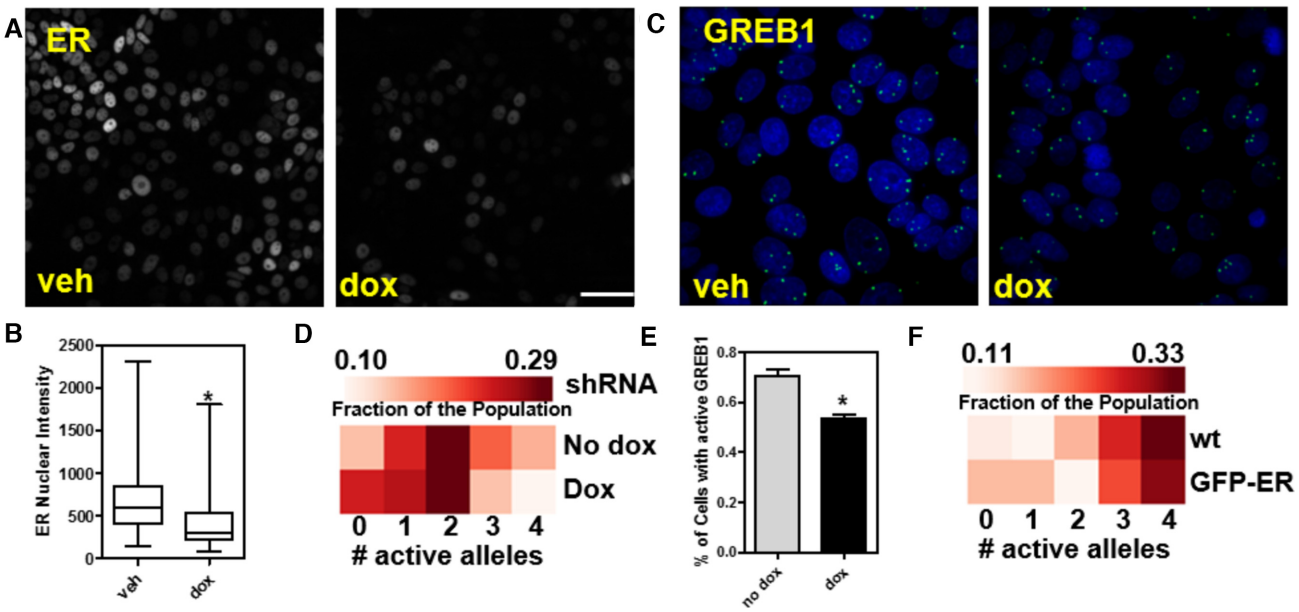

Figure 4. ER levels are not the sole determinants of allele-by-allele variation in responses to E2. (**A**, **B**) MCF-7/shER stable cells were treated with doxycycline to induce reduction in ER levels. Images were captured at 20× (scale bar: 100 μm) and quantified by automated image analysis. (**C**, **D**) GREB1 smFISH was performed in MCF-7/shER cells after 1 h of E2 treatment. Heatmap indicates fraction of cells with 0–4 GREB1 active alleles. (**E**) graph shows fraction of active cells before and after doxycycline treatment. (**F**) MCF-7 overexpressing GFP-ER were treated with E2 for 1 h before GREB1 smFISH. Heatmap indicates fraction of cells with 0–4 GREB1 active alleles.

in distribution over time as depicted by heatmaps in Figure 1B and C. For example, after a 1 h exposure to E2, for GREB1, 12% of the cells had no active alleles, 15% of cells had one, 22% of cells had two, 25% of cells had three, and 25% of cells had four, indicating a large variability in allele-by-allele responses. The same variability was true for MYC and for each individual time point (and dose of hormone, as shown below). As an ensemble measure, we also represented the same data as average number of active alleles/cell (Figure 1D) that clearly shows the different time course of allele activation between the two target genes, in keeping with RNA-seq and microarray data, and the clear lack of saturated response to hormone (i.e. all cells with all active alleles).

We also calculated the percentage of 'activated cells,' defined here as cells with two or more active alleles at each time point (Figure 1E), based on the fact that in vehicle treated cells, the vast majority of them has zero or one ac-

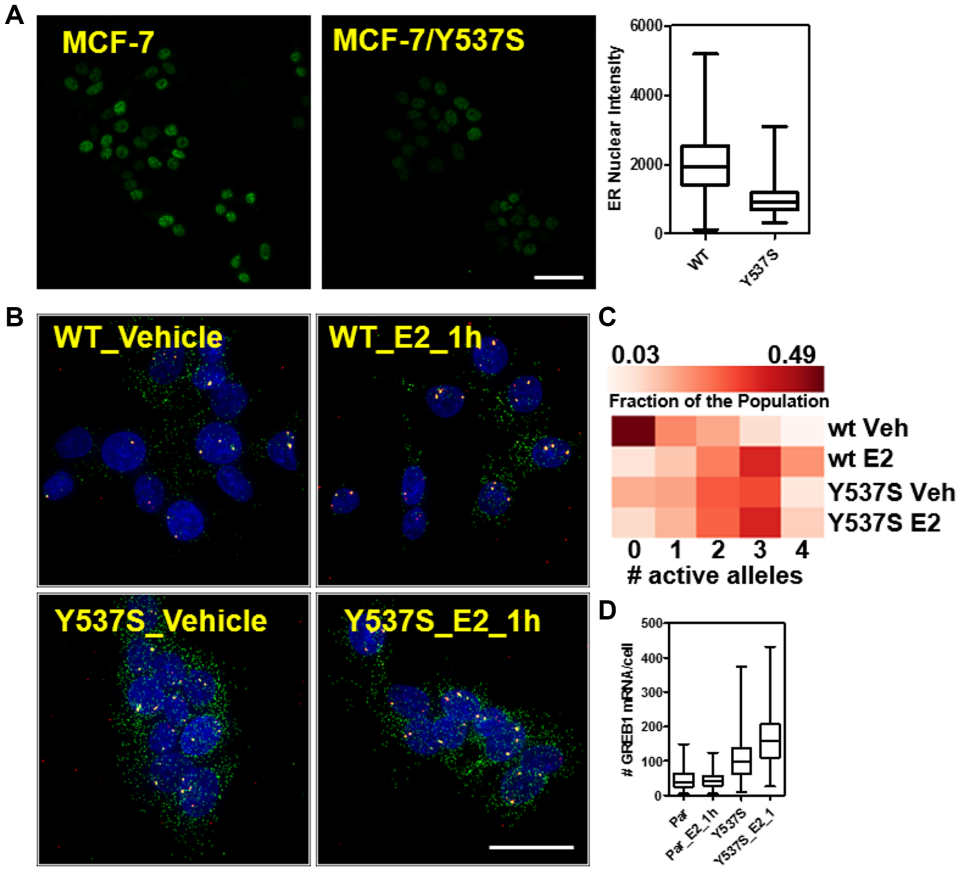

Figure 5. Constitutively active ER is not sufficient to activate all alleles simultaneously. (**A**) Representative images and box-plot quantifying ER single cell immunofluorescence in wild type and Y537S MCF-7 cells. (**B**) Representative images of GREB1 RNA FISH (exon, green; intron, red) in MCF-7 and MCF-7/ERY537S cells after vehicle or E2 1 h, scale bar 20 μm. (**C**, **D**) Quantitation (>200 cells from panel C) showing the fraction of cells containing 0–4 GREB1 active alleles, or as a box-plot with the number of mature GREB1 mRNAs/cell.

tive alleles. For example, at the 30-minute time point, compared to vehicle treated cells, the percentage of activated cells increased ∼3–5-fold for GREB1 (20–53%) and MYC (14–66%), respectively, but far from the maximum possible response (100%); while at the four hour time point, the population of activated cells reached a plateau of ∼70–80% for GREB1 while decreasing to 35% for MYC (Figure 1E), in keeping with the expected time course for both genes.

This variability in allele and cell responses was also true in dose-response experiment (E2 concentration range: 1 pM to 1 μM, Figure 1F–I), where we measured an EC_{50} of ∼10 pM after 1 h of E2 exposure for GREB1, and ∼6 pM after 30 min of treatment for MYC, comparable to bulk population assays (32). We then confirmed that the observed responses were transcription- and ER-dependent (Figure 2A) by pre-treating MCF-7 cells for 1 h prior to E2 with the well-established ER antagonists, fulvestrant and bazedoxifene; and, with two transcription inhibitors with different mechanisms, flavopiridol and actinomycin D. Indeed, as shown in the heatmap in Figure 2A, all the inhibitors completely blocked E2-mediated GREB1 stimulation.

The total number of gene loci/cell was not a determinant of the cell-to-cell or allele-by-allele response to hormone, as we observed similar differences in GREB1 activation in other breast cancer cell lines containing two (T47D), three (ZR75-1) or four (BT474) copies of the locus (Figure 2B).

This allele-by-allele response was not specific to E2, as other steroid hormones (i.e. androgens – dihydroxystestosterone (DHT), glucocorticoids – dexamethasone) and endocrine disrupting chemicals/phytoestrogens (bisphenol A (BPA) and genistein), elicited, at the 1-hour time point, similar allele-by-allele variable responses, albeit with different magnitude and distribution of active alleles for both GREB1 and MYC (Figure 2C). In the heatmaps, compounds are ordered based on clustering analysis highlighting similarities in response. For GREB1, a gene commonly stimulated by all steroid hormones, the active population (>2 active alleles/cell) was 70% for E2, between 60% and 75% for BPA ad genistein, 45% for dexamethasone and only 20% for DHT, only a slight increase compared to 13% in vehicle treated cells. In the case of DHT, GREB1 stimulation is delayed, starting to ramp up after 4 h of treatment (data not shown). For MYC, the active population was around 50% for E2 treatment (at 1 h), with BPA being very similar and genistein showing higher activity. However, both dexamethasone and DHT were completely inactive; confirming the gene specific effects of steroid hormones.

As expected from many other studies in disparate cell models (12,17,25), the cell-to-cell variation was also true

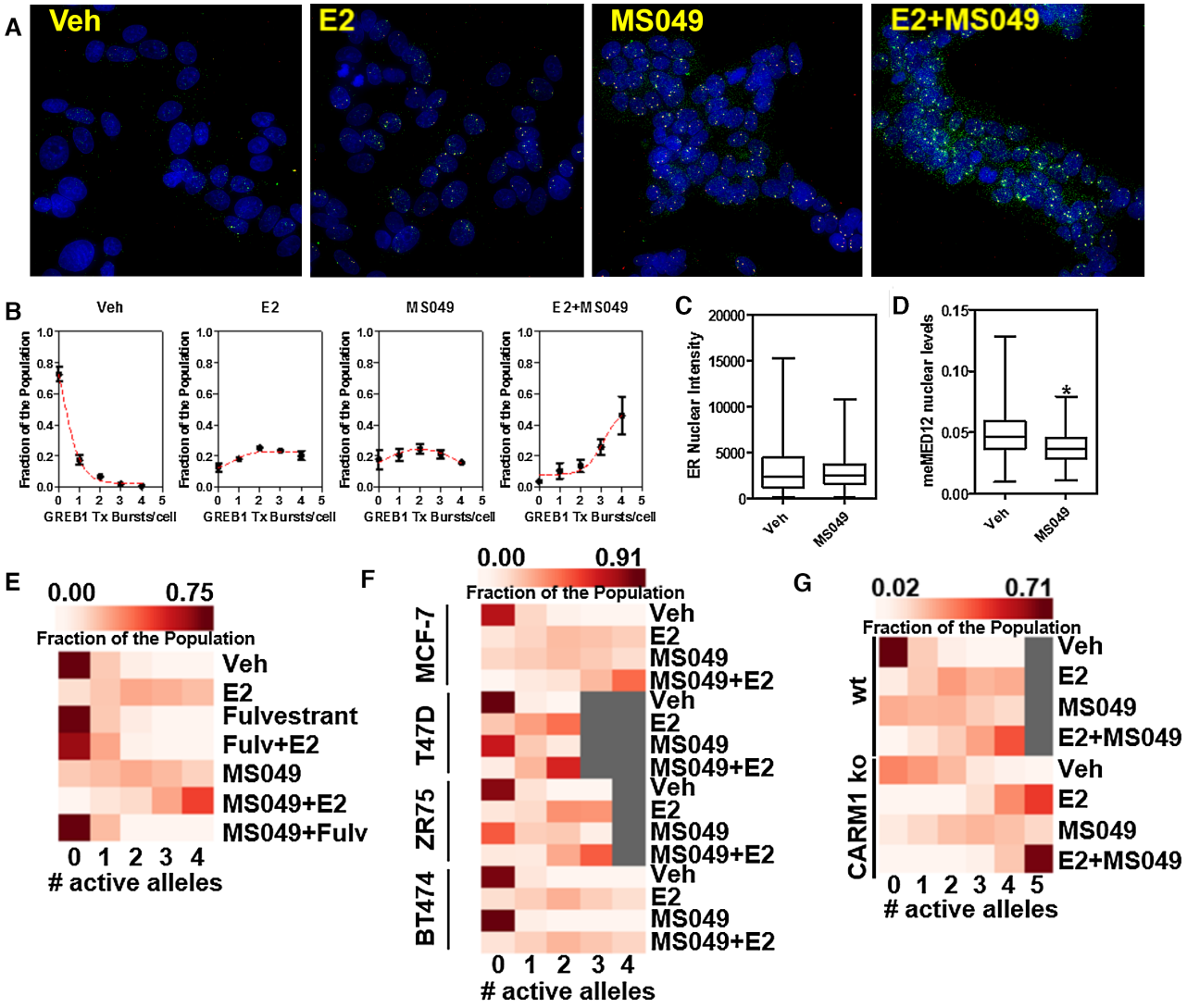

Figure 6. The CARM1 and PRMT6 inhibitor MS049 enhances ER-mediated GREB1 induction. (**A**) Representative images of GREB1 smFISH in MCF-7 cells treated with MS049 (10 μM, overnight pretreatment) with or without E2 10 nM for 1 h. (**B**) Data shows the fraction ± standard deviation of cells with 0–4 active GREB1 alleles (eight independent experiments). (**C**) single cell quantitation of ER levels after vehicle or MS049 treatment. (**D**) single cell quantitation of methylated MED12 after vehicle or MS049 treatment. (**E**) Heatmap showing distribution of GREB1 active alleles in MCF-7 treated with the indicated combinations of compounds. (**F**) Multiple cell lines were treated with MS049 with and without E2 10nM for 1 h and smFISH for GREB1 was performed. Data is represented as a heatmap. (**G**) smRNA GREB1 FISH quantitation of MCF-7 wt and MCF-7/CARM1 KO cells after treatments. Scale bar for all images is 10 μm.

for both GREB1 and MYC steady state RNA as measured by counting the number of mRNA particles (marked by exon-specific probes) per cell (Figure 2D). In keeping with microarray, RNA-seq data and transcriptionally active alleles/cell, the time course of E2 response was also different between the two target genes, being sustained for GREB1 and transient for MYC, but with a delayed response as compared to allele activation, as expected.

ER levels alone do not fully explain allele-by-allele gene regulation

We sought to determine if the variability of response to hormone was simply the result of cell-to-cell differences in ER protein levels. First, we performed immunofluorescence and single cell analysis of ER expression in MCF-7 cells and found to be >100-fold difference between cells (Figure 3A, inset shows box-plot analysis of >85 000 cells). Importantly, the cell-to-cell variation in ER levels was not epitope-dependent as co-immunolabeling with three different ER antibodies showed high correlation ($r > 0.9$, Supplementary Figure S1A and B). To establish a direct relationship between ER nuclear levels and gene activation, we first optimized the IF/FISH protocol, using a novel high throughput hybridoma screen (33), to identify antibodies that would work comparably following RNA FISH protocols, ultimately identifying two antibodies that can be used in this assay as described in materials and methods.

We performed IF/FISH for ER and both GREB1 and MYC after 1 h and 30 min of E2 treatment, respectively

(Figure 3B), and imaged them with semi-automated deconvolution microscopy.

In Figure 3C, we stratified cells based on the number of active alleles and determined the ER levels for each class. We found poor correlation (Spearman's) between ER levels and the number of active GREB1 or MYC alleles ($r = 0.16$–0.18). However, by ANOVA, there is a statistically higher ER level in cells that have the highest number of active alleles for both genes. We then divided the cell population based on ER levels as low (below 25th percentile), medium (25th–75th) and high (above 75th) and evaluated the fraction of each subpopulation containing 0–4 active alleles for GREB1 or MYC (Figure 3D). For GREB1, there was no difference in the active cell population (>60%) between cells with medium or high levels of ER; however, cells in the bottom 25th percentile for ER expression showed a reduced response (Figure 3D) with 47% active cells, largely due to a 50% reduction is cells with all four active alleles. A very similar situation was observed for MYC.

In keeping with the above observations, transiently lowering ER levels (∼50% in the total cell population, Figure 4A and B) with an inducible, stable shRNA, reduced the fraction of responding cells (50% versus 70% at 1 h, Figure 4C–E) and changed the distribution of the number of active alleles in the population. Interestingly, the bottom 25th percentile of the shRNA (dox-treated) cells, which contains ∼5% of ER expressed in the wild type population, still showed E2 induction of GREB1, with ∼25% of cells with two or more actively-firing alleles, further indicating that very little ER protein per cell is needed to initiate transcriptional responses, whereas higher levels are required for maximal responsiveness. Importantly, the opposite was not true, as overexpression of GFP-ER did not change the fraction of active GREB1 alleles after hormone stimulation (Figure 4F).

Constitutively active ER is not sufficient to maximize hormonal responses

Because ER levels alone did not explain the cell-to-cell variation in GREB1 activation, we used CRISPR/Cas9 to knock-in the Y537S mutation in the ER gene, which has been shown to render the receptor constitutively active (34–36), thus directly querying if the 'activation status' of ER was the main controlling factor. The homozygous ER/Y537S MCF-7 cell line expressed <50% of the levels of ER compared to wild type cells (Figure 5A), in keeping with previous observations showing that Y537S mutant has higher protein turnover rate (37).

In the ER/Y537S cell line we observed, as expected, a ligand-independent activation of GREB1, similar to wild type cells after 1 hour of E2 treatment (Figure 5B and C). However, the distribution of the number of active GREB1 alleles between cells was comparable to E2-treated wild type cells, without reaching full activation capacity. The same was also true for mature mRNA levels (Figure 5D). This indicated that while ER levels and activation status are essential for stimulating GREB1 transcription, they are not the only parameters controlling allele-by-allele variation during the hormonal response, as no maximal response (i.e. all alleles active) is observed by either the Y537S mutant alone, or after E2 treatment.

The small molecule MS049 enhances ER-mediated allele-by-allele responses

As ER-regulated transcription depends upon the dynamic recruitment of coregulator complexes (6,38,39), we sought to determine if their activity would be important in modulating the allele-by-allele response to hormone. We developed and used a high throughput microscopy-based ER/GREB1 IF/FISH approach to test ∼60 small molecule inhibitors (SMIs) from several classes of epigenetic modulators. Surprisingly, a few compounds increased the fraction of E2-induced GREB1 active alleles, indicating that mechanisms exist to control the magnitude of the hormonal response through allelic regulation. In this study, we focused on MS049, an inhibitor of two protein methyl arginine methyltransferases, CARM1 and PRMT6 (40), both of which have been linked to ER activity (41–44). We found that combining MS049 with E2 increased the fraction of active cells (86% versus 69%) while more than doubling the fraction of cells with four active alleles (46% versus 20%) (Figure 6A and B), with no change in ER levels (Figure 6C). Interestingly, MS049 treatment without hormone addition was also capable of activating GREB1 transcription in an ER-dependent manner (Figure 6E) as demonstrated by complete block of its action by cotreatment with the ER antagonist fulvestrant. MS049 was further validated by measuring the nuclear level of methylated MED12, a *bona fide* CARM1 direct target (Figure 6D) (45). However, MS049 did not promote direct ER binding to DNA, as evidenced by the lack of response in an ER biosensor cell line (46,47) (Supplementary Figure S2) where stable expression of GFP-ER that targets an engineered multi-copy visible array of the estrogen-responsive prolactin gene only when treated with E2, or any known estrogenic or anti-estrogenic compound. Testing MS049 in other ER positive breast cancer cell models revealed that the effects were consistent across cell lines, except in Her2-overexpressing BT474 cells, where no effect was observed, possibly indicating that cell specific signaling pathways might play a role in controlling the effect of the methyltransferase inhibitor (Figure 6F). Also, importantly MS049 had no effect on MYC induction, suggesting a gene-specific mechanism of action. As we recently published a CARM1 ChiP-seq dataset in MCF-7 cells treated with E2 (45), we checked if there were any differences in CARM1 recruitment to the MYC and GREB1 loci. Genome browser tracks (Supplementary Figure S2D) clearly highlight major CARM1 peaks only at the GREB1 locus, strengthening the notion that the gene specific effects of MS049 can be linked to CARM1 genomic localization. To determine if MS049 was acting mainly through CARM1, we employed MCF-7 CARM1 knock-out cells (48) that, interestingly, have acquired a fifth copy of the GREB1 locus and express higher ER protein (2.5 fold, Supplementary Figure S2C) than wild type MCF-7. Further, GREB1 alleles were basally more active in CARM1 KO cells (41% versus 12%), and this increased after E2 treatment (94% versus 73% with two or more active alleles) (Figure 6G). Importantly, loss of CARM1 partially mim-

icked the effect of MS049 in wild type cells (41% versus 54% active cells), suggesting a novel role for CARM1 in controlling allele specific transcriptional activation. However, the fraction of active alleles still increased when CARM1 KO cells were treated with MS049, indicating that PRMT6 and/or other unrelated factors also likely play a role.

DISCUSSION

In this study, we examined the effects on steroid hormones, specifically of estrogens, on target genes with different gene structure and time-course of stimulation, at the single cell and single allele level in breast cancer cells. By using single molecule RNA FISH, we simultaneously measured the cell-to-cell variability of steady state RNA and, more interestingly, in allele-by-allele responses in the same cell, to monitor two estrogen receptor target genes, GREB1 and MYC. The choice of these two genes stems from studies (3,26) that showed them as primary ER targets with very different gene length and intron/exon structure, and with distinct temporal stimulation patterns, with MYC being a transient response, while GREB1 exhibits a more sustained response over time. Through time- and dose-series, we showed that hormone activation occurs quickly (15 min or earlier), in line with GRO-seq data (3). Importantly, smRNA FISH afforded us the opportunity to determine cell to cell variation, but also directly measure the number of active alleles/cell. We found that all cells did not respond synchronously to hormone simulation (i.e. one allele at a time), and they also never reached capacity both in terms of fraction of active cells (defined as having two or more active alleles, maximum was 80% in the time frame studied) or number of active alleles/cell (reaching a maximum lower than three/cell for GREB1, which has four alleles in MCF-7 cells). This was true for both genes studied and independent of the cell model, number of alleles/cell and stimulant tested, whether natural or synthetic.

We then explored the impact of ER levels on the allele-by-allele regulation of its target genes by performing correlative studies via immunofluorescence/RNA FISH, by down-regulating and overexpressing ER, and finally by generating a constitutively active endogenous ER via CRISPR/Cas9 to introduce the Y537S mutation in the endogenous alleles. The combination of these studies highlighted the fact that neither the level or the activation status of the receptor is the main determinant of allele-by-allele variation, as probably best demonstrated in the Y537S mutant cell line where there is lower ER expression and the allele-by-allele variation is virtually identical to estrogen-treated wild type cells.

After DNA binding, ER serves as a platform for many coregulator complexes (6) that alter chromatin structure and facilitate transcription initiation (49). For this reason, we performed a survey of small molecule inhibitors of epigenetic modulators (mostly HDAC, KDM and KAT inhibitors) and identified MS049, a PRMT6/CARM1 inhibitor, as capable of increasing the number of active alleles/cell after hormone stimulation (roughly doubling the number of cells with max active alleles), in an ER-dependent manner and specifically for GREB1. We validated the inhibitor action by using CARM1 knock-out MCF-7 cells and monitoring methylated MED12, a component of the Mediator complex recently identified as a central component of CARM1-mediated transcriptional activation (45).

In conclusion, we present a heretofore unrecognized regulatory mode of hormone/nuclear receptor-induced gene transcription at the single cell and allele level. We further show that the variation in allele-by-allele responses is not directly linked to ER protein levels. More importantly, the inability of a constitutively active ER to cause activation of all GREB1 alleles in every cell indicates that mechanisms exist to fine-tune responses to hormone independently of the receptor activation status.

This study also highlights a new role for nuclear receptor coregulators in controlling hormone-dependent gene transcription. We suggest that protein arginine methyltransferases may play an important, previously unrecognized role in fine-tuning hormonal responses, maintaining both cell-to-cell variability (which is evolutionarily advantageous) and preventing saturation of responses at the single cell and/or population levels. The mechanistic underpinning of their action warrants further exploration and may include modulation by intracellular signaling pathways, post-translational modifications, chromatin remodeling and DNA repair, and/or assembly/disassembly dynamics of coregulator complexes (42). These new observations further advance the notion of nuclear receptor coactivators as multi-functional components of dynamic large protein complexes that participate in a myriad of expected and, as shown here, novel mechanistic processes that regulate hormonal control of gene expression.

SUPPLEMENTARY DATA

Supplementary Data are available at NAR Online.

ACKNOWLEDGEMENTS

We would like to thank Dr Julien Dubrulle for fruitful discussions on the project, and Raymund Yin (LGC Biosearch Technologies) for assistance in RNA FISH probe set design, Dr Ido Golding (BCM), Dr Gary Chamness (BCM) and Dr Z. David Sharp (UT San Antonio) for critically reading the manuscript.

FUNDING

M.A.M. is supported by an NIH/NIEHS Superfund grant [P42ES027704]; M.A.M. and F.S. are supported via the CPRIT-funded GCC Center for Advanced Microscopy and Image Informatics [RP170719]; M.T.B. is supported by NIH [GM126421]; S.A.W.F. by NIH [R01-CA72038]; CPRIT [RP120732]; Breast Cancer Research Foundation; R.S. by the Breast Cancer Research Foundation, NIH Breast Cancer Specialized Programs of Research Excellence Grants [P50CA058183, P50CA186784]; S.G.K. for the Cure Foundation Promise Grant [PG12221410]; Imaging was supported by the Integrated Microscopy Core at Baylor College of Medicine with funding from NIH [DK56338, CA125123]; CPRIT [RP150578]; Dan L. Duncan Comprehensive Cancer Center, and the John S. Dunn Gulf Coast

Consortium for Chemical Genomics; The Gulf Coast Consortium for Chemical Genomics high throughput screening center is funded by CPRIT [RP110532, RP150578]. Funding for open access charge: CPRIT [RP170719].
Conflict of interest statement. Hans E. Johansson is an employee of LGC Biosearch Technologies.

REFERENCES

1. Green,K.A. and Carroll,J.S. (2007) Oestrogen-receptor-mediated transcription and the influence of co-factors and chromatin state. *Nat. Rev. Cancer*, **7**, 713–722.
2. Heldring,N., Pike,A., Andersson,S., Matthews,J., Cheng,G., Hartman,J., Tujague,M., Strom,A., Treuter,E., Warner,M. *et al.* (2007) Estrogen receptors: how do they signal and what are their targets. *Physiol. Rev.*, **87**, 905–931.
3. Hah,N., Danko,C.G., Core,L., Waterfall,J.J., Siepel,A., Lis,J.T. and Kraus,W.L. (2011) A rapid, extensive, and transient transcriptional response to estrogen signaling in breast cancer cells. *Cell*, **145**, 622–634.
4. Ross-Innes,C.S., Stark,R., Teschendorff,A.E., Holmes,K.A., Ali,H.R., Dunning,M.J., Brown,G.D., Gojis,O., Ellis,I.O., Green,A.R. *et al.* (2012) Differential oestrogen receptor binding is associated with clinical outcome in breast cancer. *Nature*, **481**, 389–393.
5. Carroll,J.S., Meyer,C.A., Song,J., Li,W., Geistlinger,T.R., Eeckhoute,J., Brodsky,A.S., Keeton,E.K., Fertuck,K.C., Hall,G.F. *et al.* (2006) Genome-wide analysis of estrogen receptor binding sites. *Nat. Genet.*, **38**, 1289–1297.
6. Foulds,C.E., Feng,Q., Ding,C., Bailey,S., Hunsaker,T.L., Malovannaya,A., Hamilton,R.A., Gates,L.A., Zhang,Z., Li,C. *et al.* (2013) Proteomic analysis of coregulators bound to ERα on DNA and nucleosomes reveals coregulator dynamics. *Mol. Cell*, **51**, 185–199.
7. Bolt,M.J., Stossi,F., Callison,A.M., Mancini,M.G., Dandekar,R. and Mancini,M.A. (2015) Systems level-based RNAi screening by high content analysis identifies UBR5 as a regulator of estrogen receptor-alpha protein levels and activity. *Oncogene*, **34**, 154–164.
8. Zhu,D., Zhao,Z., Cui,G., Chang,S., Hu,L., See,Y.X., Lim,M.G.L., Guo,D., Chen,X., Robson,P. *et al.* (2018) Single-cell transcriptome analysis reveals estrogen signaling coordinately augments one-carbon, polyamine, and purine synthesis in breast cancer. *Cell Rep.*, **25**, 2285–2298.
9. Rodriguez,J., Ren,G., Day,C.R., Zhao,K., Chow,C.C. and Larson,D.R. (2019) Intrinsic dynamics of a human gene reveal the basis of expression heterogeneity. *Cell*, **176**, 213–226.
10. Sepúlveda,L.A., Xu,H., Zhang,J., Wang,M. and Golding,I. (2016) Measurement of gene regulation in individual cells reveals rapid switching between promoter states. *Science*, **351**, 1218–1222.
11. Padovan-Merhar,O., Nair,G.P., Biaesch,A.G., Mayer,A., Scarfone,S., Foley,S.W., Wu,A.R., Churchman,L.S., Singh,A. and Raj,A. (2015) Single mammalian cells compensate for differences in cellular volume and DNA copy number through independent global transcriptional mechanisms. *Mol. Cell*, **58**, 339–352.
12. Raj,A., Peskin,C.S., Tranchina,D., Vargas,D.Y. and Tyagi,S. (2006) Stochastic mRNA synthesis in mammalian cells. *PLoS Biol.*, **4**, e309.
13. Bahar Halpern,K., Tanami,S., Landen,S., Chapal,M., Szlak,L., Hutzler,A., Nizhberg,A. and Itzkovitz,S. (2015) Bursty gene expression in the intact mammalian liver. *Mol. Cell*, **58**, 147–156.
14. Coulon,A., Chow,C.C., Singer,R.H. and Larson,D.R. (2013) Eukaryotic transcriptional dynamics: from single molecules to cell populations. *Nat. Rev. Genet.*, **14**, 572–584.
15. Skinner,S.O., Xu,H., Nagarkar-Jaiswal,S., Freire,P.R., Zwaka,T.P. and Golding,I. (2016) Single-cell analysis of transcription kinetics across the cell cycle. *Elife*, **5**, e12175.
16. Bahar Halpern,K., Caspi,I., Lemze,D., Levy,M., Landen,S., Elinav,E., Ulitsky,I. and Itzkovitz,S. (2015) Nuclear retention of mRNA in Mammalian tissues. *Cell Rep.*, **13**, 2653–2662.
17. Battich,N., Stoeger,T. and Pelkmans,L. (2015) Control of transcript variability in single mammalian cells. *Cell*, **163**, 1596–1610.
18. Guantes,R., Rastrojo,A., Neves,R., Lima,A., Aguado,B. and Iborra,F.J. (2015) Global variability in gene expression and alternative splicing is modulated by mitochondrial content. *Genome Res.*, **25**, 633–644.
19. das Neves,R.P., Jones,N.S., Andreu,L., Gupta,R., Enver,T. and Iborra,F.J. (2010) Connecting variability in global transcription rate to mitochondrial variability. *PLoS Biol.*, **8**, e1000560.
20. Bartman,C.R., Hsu,S.C., Hsiung,C.C.-S., Raj,A. and Blobel,G.A. (2016) Enhancer regulation of transcriptional bursting parameters revealed by forced chromatin looping. *Mol. Cell*, **62**, 237–247.
21. Senecal,A., Munsky,B., Proux,F., Ly,N., Braye,F.E., Zimmer,C., Mueller,F. and Darzacq,X. (2014) Transcription factors modulate c-fos transcriptional bursts. *Cell Rep.*, **8**, 75–83.
22. Kalo,A., Kanter,I., Shraga,A., Sheinberger,J., Tzemach,H., Kinor,N., Singer,R.H., Lionnet,T. and Shav-Tal,Y. (2015) Cellular levels of signaling factors are sensed by β-actin alleles to modulate transcriptional pulse intensity. *Cell Rep.*, **11**, 419–432.
23. Lee,R.E.C., Walker,S.R., Savery,K., Frank,D.A. and Gaudet,S. (2014) Fold change of nuclear NF-κB determines tnf-induced transcription in single cells. *Mol. Cell*, **53**, 867–879.
24. Pejerrey,S.M., Dustin,D., Kim,J.-A., Gu,G., Rechoum,Y. and Fuqua,S.A.W. (2018) The impact of ESR1 mutations on the treatment of metastatic breast cancer. *Horm. Cancer*, **9**, 215–228.
25. Shah,S., Takei,Y., Zhou,W., Lubeck,E., Yun,J., Eng,C.-H.L., Koulena,N., Cronin,C., Karp,C., Liaw,E.J. *et al.* (2018) Dynamics and spatial genomics of the nascent transcriptome by intron seqFISH. *Cell*, **174**, 363–376.
26. Frasor,J., Danes,J.M., Komm,B., Chang,K.C.N., Lyttle,C.R. and Katzenellenbogen,B.S. (2003) Profiling of estrogen up- and down-regulated gene expression in human breast cancer cells: insights into gene networks and pathways underlying estrogenic control of proliferation and cell phenotype. *Endocrinology*, **144**, 4562–4574.
27. Dubik,D., Dembinski,T.C. and Shiu,R.P. (1987) Stimulation of c-myc oncogene expression associated with estrogen-induced proliferation of human breast cancer cells. *Cancer Res.*, **47**, 6517–6521.
28. Ghosh,M.G., Thompson,D.A. and Weigel,R.J. (2000) PDZK1 and GREB1 are estrogen-regulated genes expressed in hormone-responsive breast cancer. *Cancer Res.*, **60**, 6367–6375.
29. Nwachukwu,J.C., Srinivasan,S., Zheng,Y., Wang,S., Min,J., Dong,C., Liao,Z., Nowak,J., Wright,N.J., Houtman,R. *et al.* (2016) Predictive features of ligand-specific signaling through the estrogen receptor. *Mol. Syst. Biol.*, **12**, 864.
30. Kocanova,S., Kerr,E.A., Rafique,S., Boyle,S., Katz,E., Caze-Subra,S., Bickmore,W.A. and Bystricky,K. (2010) Activation of estrogen-responsive genes does not require their nuclear co-localization. *PLoS Genet.*, **6**, e1000922.
31. Rummukainen,J., Kytölä,S., Karhu,R., Farnebo,F., Larsson,C. and Isola,J.J. (2001) Aberrations of chromosome 8 in 16 breast cancer cell lines by comparative genomic hybridization, fluorescence in situ hybridization, and spectral karyotyping. *Cancer Genet. Cytogenet.*, **126**, 1–7.
32. Dahlman-Wright,K., Cavailles,V., Fuqua,S.A., Jordan,V.C., Katzenellenbogen,J.A., Korach,K.S., Maggi,A., Muramatsu,M., Parker,M.G. and Gustafsson,J.-A. (2006) International union of pharmacology. LXIV. estrogen receptors. *Pharmacol. Rev.*, **58**, 773–781.
33. Szafran,A.T., Mancini,M.G., Nickerson,J.A., Edwards,D.P. and Mancini,M.A. (2016) Use of HCA in subproteome-immunization and screening of hybridoma supernatants to define distinct antibody binding patterns. *Methods*, **96**, 75–84.
34. Weis,K.E., Ekena,K., Thomas,J.A., Lazennec,G. and Katzenellenbogen,B.S. (1996) Constitutively active human estrogen receptors containing amino acid substitutions for tyrosine 537 in the receptor protein. *Mol. Endocrinol.*, **10**, 1388–1398.
35. Harrod,A., Fulton,J., Nguyen,V.T.M., Periyasamy,M., Ramos-Garcia,L., Lai,C.-F., Metodieva,G., de Giorgio,A., Williams,R.L., Santos,D.B. *et al.* (2016) Genomic modelling of the ESR1 Y537S mutation for evaluating function and new therapeutic approaches for metastatic breast cancer. *Oncogene*, **36**, 2286–2296.
36. Gelsomino,L., Gu,G., Rechoum,Y., Beyer,A.R., Pejerrey,S.M., Tsimelzon,A., Wang,T., Huffman,K., Ludlow,A., Andò,S. *et al.* (2016) ESR1 mutations affect anti-proliferative responses to tamoxifen through enhanced cross-talk with IGF signaling. *Breast Cancer Res. Treat.*, **157**, 253–265.
37. Sun,J., Zhou,W., Kaliappan,K., Nawaz,Z. and Slingerland,J.M. (2012) ERα phosphorylation at Y537 by src triggers E6-AP-ERα

binding, ERα Ubiquitylation, promoter occupancy, and target gene expression. *Mol. Endocrinol.*, **26**, 1567–1577.
38. Stenoien,D.L., Nye,A.C., Mancini,M.G., Patel,K., Dutertre,M., O'Malley,B.W., Smith,C.L., Belmont,A.S. and Mancini,M.A. (2001) Ligand-mediated assembly and real-time cellular dynamics of estrogen receptor -coactivator complexes in living cells. *Mol. Cell Biol.*, **21**, 4404–4412.
39. Métivier,R., Penot,G., Hübner,M.R., Reid,G., Brand,H., Kos,M. and Gannon,F. (2003) Estrogen receptor-alpha directs ordered, cyclical, and combinatorial recruitment of cofactors on a natural target promoter. *Cell*, **115**, 751–763.
40. Shen,Y., Szewczyk,M.M., Eram,M.S., Smil,D., Kaniskan,H.Ü., Ferreira de Freitas,R., Senisterra,G., Li,F., Schapira,M., Brown,P.J. *et al.* (2016) Discovery of a potent, selective, and cell-active dual inhibitor of protein arginine methyltransferase 4 and protein arginine methyltransferase 6. *J. Med. Chem.*, **59**, 9124–9139.
41. Chen,D., Huang,S.M. and Stallcup,M.R. (2000) Synergistic, p160 coactivator-dependent enhancement of estrogen receptor function by CARM1 and p300. *J. Biol. Chem.*, **275**, 40810–40816.
42. Feng,Q., Yi,P., Wong,J. and O'Malley,B.W. (2006) Signaling within a coactivator complex: methylation of SRC-3/AIB1 is a molecular switch for complex disassembly. *Mol. Cell Biol.*, **26**, 7846–7857.
43. Sun,Y., Chung,H.H., Woo,A.R.E. and Lin,V.C.-L. (2014) Protein arginine methyltransferase 6 enhances ligand-dependent and -independent activity of estrogen receptor α via distinct mechanisms. *Biochim. Biophys. Acta - Mol. Cell Res.*, **1843**, 2067–2078.
44. Harrison,M.J., Tang,Y.H. and Dowhan,D.H. (2010) Protein arginine methyltransferase 6 regulates multiple aspects of gene expression. *Nucleic Acids Res.*, **38**, 2201–2216.
45. Cheng,D., Vemulapalli,V., Lu,Y., Shen,J., Aoyagi,S., Fry,C.J., Yang,Y., Foulds,C.E., Stossi,F., Treviño,L.S. *et al.* (2018) CARM1 methylates MED12 to regulate its RNA-binding ability. *Life Sci. Alliance*, **1**, e201800117.
46. Sharp,Z.D., Mancini,M.G., Hinojos,C.A., Dai,F., Berno,V., Szafran,A.T., Smith,K.P., Lele,T.P., Lele,T.T., Ingber,D.E. *et al.* (2006) Estrogen-receptor-alpha exchange and chromatin dynamics are ligand- and domain-dependent. *J. Cell Sci.*, **119**, 4101–4116.
47. Stossi,F., Bolt,M.J., Ashcroft,F.J., Lamerdin,J.E., Melnick,J.S., Powell,R.T., Dandekar,R.D., Mancini,M.A.G.M.A., Walker,C.L., Westwick,J.K. *et al.* (2014) Defining estrogenic mechanisms of bisphenol A analogs through high throughput microscopy-based contextual assays. *Chem. Biol.*, **21**, 743–753.
48. Wang,L., Zhao,Z., Meyer,M.B., Saha,S., Yu,M., Guo,A., Wisinski,K.B., Huang,W., Cai,W., Pike,J.W. *et al.* (2014) CARM1 methylates chromatin remodeling factor BAF155 to enhance tumor progression and metastasis. *Cancer Cell*, **25**, 21–36.
49. Gates,L.A., Gu,G., Chen,Y., Rohira,A.D., Lei,J.T., Hamilton,R.A., Yu,Y., Lonard,D.M., Wang,J., Wang,S.-P. *et al.* (2018) Proteomic profiling identifies key coactivators utilized by mutant ERα proteins as potential new therapeutic targets. *Oncogene*, **37**, 4581–4598.
50. Meerbrey,K.L., Hu,G., Kessler,J.D., Roarty,K., Li,M.Z., Fang,J.E., Herschkowitz,J.I., Burrows,A.E., Ciccia,A., Sun,T. *et al.* (2011) The pINDUCER lentiviral toolkit for inducible RNA interference in vitro and in vivo. *Proc. Natl. Acad. Sci. U.S.A.*, **108**, 3665–3670.
51. Fu,X., Creighton,C.J., Biswal,N.C., Kumar,V., Shea,M., Herrera,S., Contreras,A., Gutierrez,C., Wang,T., Nanda,S. *et al.* (2014) Overcoming endocrine resistance due to reduced PTEN levels in estrogen receptor-positive breast cancer by co-targeting mammalian target of rapamycin, protein kinase B, or mitogen-activated protein kinase kinase. *Breast Cancer Res.*, **16**, 430.
52. Orjalo,A.V. and Johansson,H.E. (2016) Stellaris® RNA fluorescence In situ hybridization for the simultaneous detection of immature and mature long noncoding RNAs in adherent cells. *Methods Mol. Biol.*, **1402**, 119–134.
53. Stossi,F., Dandekar,R.D., Bolt,M.J., Newberg,J.Y., Mancini,M.A.M.G., Kaushik,A.K., Putluri,V., Sreekumar,A. and Mancini,M.A.M.G. (2016) High throughput microscopy identifies bisphenol AP, a bisphenol A analog, as a novel AR down-regulator. *Oncotarget*, **7**, 16962–16974.
54. Szafran,A.T. and Mancini,M.A. (2014) The myImageAnalysis project: a web-based application for high-content screening. *Assay Drug Dev. Technol.*, **12**, 87–99.
55. Demsar,J., Curk,T., Erjavec,A., Gorup,C., Hocevar,T., Milutinovic,M., Mozina,M., Polajnar,M., Toplak,M., Staric,A. *et al.* (2013) Orange: data mining toolbox in python. *J. Mach. Learn. Res.*, **14**, 2349–2353.